Laser performance and thermal lens of diode-pumped Nd, Y-codoped:SrF_2 single crystals

Jie Guo (郭 洁)[1], Jinfeng Li (李进峰)[1], Peng Gao (高 鹏)[1], Liangbi Su (苏良碧)[2], Jun Xu (徐 军)[2], and Xiaoyan Liang (梁晓燕)[1,3*]

[1]*Shanghai Institute of Optics and Fine Mechanics, Chinese Academy of Sciences, Shanghai 201800, China*

[2]*Shanghai Institute of Ceramics, Chinese Academy of Sciences, Shanghai 2000500, China*

[3]*School of Physical Science and Technology, Shanghai Tech University, Shanghai 200031, China*

[*]*Corresponding author: liangxy@siom.ac.cn*

Received July 16, 2014; accepted October 24, 2014; posted online November 20, 2014

We demonstrate the laser performances of Nd, Y:SrF_2 crystals with Nd^{3+} concentrations of 0.15 and 0.43 at.%. The sample with 0.43 at.% Nd^{3+} concentration yields a maximum output power of 1.023 W at 1056.9 nm with a slope efficiency of 53%. The focal length of the thermal lens is analyzed for the 0.15 at.% Nd^{3+}-doped crystal sample. An improved cavity is designed considering the thermal lens. The maximum output power is 464 mW at 1056.9 nm, with a slope efficiency of 36.1%. The wavelength is tuned within the range of 1049.74–1059.13 nm.

OCIS codes: 140.3580, 140.3530, 140.6810.

doi: 10.3788/COL201412.121403.

Diode-pumped solid-state lasers (DPSSLs) have attracted increasing attention in the past few decades as they are highly efficient, stable, compact, and cost-effective laser sources[1]. Given the enhanced reliability and performance of DPSSLs, they are applied in the scientific, industrial, and military fields[2]. Among a variety of optical materials used for DPSSLs, Nd-doped crystals are widely recognized as significant potential ones[3,4], because they provide access to the 1 μm spectral region, where directly diode-pumped lasers with outstanding performances are available. Nd-doped crystals possess large emission cross sections and long upper level lifetimes.

Efforts to search for new single crystals with high quality and optimized performance for DPSSLs have never come to an end. Nd-doped fluoride crystals attracted attention in the early years of development of the lasers due to their specific spectroscopic properties, such as broad absorption, fluorescence spectra, and long radiative lifetime of the $^4F_{3/2}$ state[5,6]. However, these crystals are not widely used mainly because of the concentration quenching caused by the aggregation of the Nd^{3+} active ions in the form of complicated "clusters"[7–9]. These clusters result in energy transfers (e.g., cross-relaxation and up-conversion) between the ions, thereby reducing the Nd^{3+} fluorescence. The problem of concentration quenching can be improved by codoping of crystals with inactive ions (e.g., Y^{3+} or La^{3+}) to "break" the clusters and improve the quantum yields; these yields were improved by reducing the interionic energy transfers. These efforts were not very successful at first, because the lasers were generally pumped by flash-lamps. However, when the laser diode (LD) pumping was widely adopted, improved performances of Nd-doped fluoride crystal-based lasers were obtained. Liu *et al.* demonstrated the continuous wave (CW) and Q-switched operations of a 0.65 at.% Nd, 10 at.% Y-codoped CaF_2–SrF_2 mixed crystal with an output power of 724 mW (CW), slope efficiency of 23.7%, and maximum pulse energy of 42.1 μJ at 1056 nm (Q-switched)[10]. Jelinek *et al.* demonstrated the pulsed and CW laser operations of temperature gradient technique (TGT)-grown Nd, Y-codoped:SrF_2 single crystals; the maximum average output power was 75 mW in the pulsed pumping regime and 380 mW at 1057 nm in the actual CW operation with a slope efficiency of 28%[11]. Qin *et al.* demonstrated the mode-locked operation of Nd, Y:CaF_2 disordered crystals with pulse widths of as low as 103 fs and an average output power of 85 mW[12]. However, the output efficiencies of Nd, Y-codoped crystals were unsatisfactory. Given this problem, the laser performances and thermal lens effect of Nd, Y-codoped:SrF_2 crystal are experimentally investigated to propose methods that increase the output efficiency.

The crystal samples were provided by Shanghai Institute of Ceramics (Shanghai, China). Figures 1 and 2 show

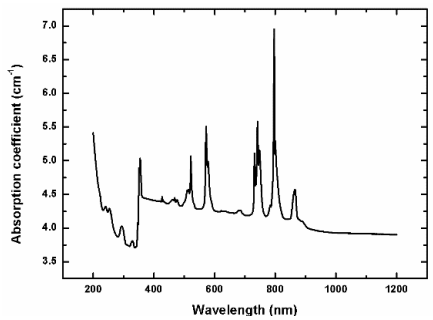

Fig. 1. Room-temperature absorption spectrum of Nd, Y-codoped:SrF_2 crystals with Nd^{3+} doping concentrations of 0.43 at.%.

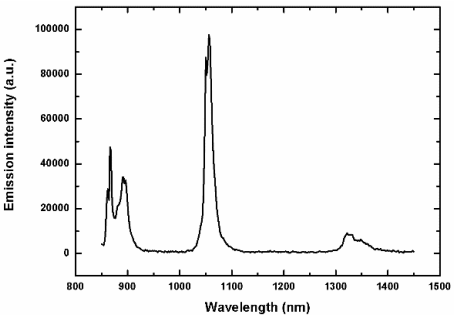

Fig. 2. Room-temperature emission spectrum of Nd, Y-codoped: SrF_2 crystals.

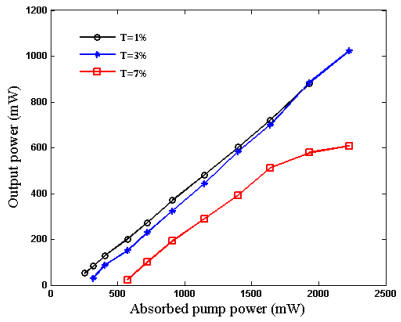

Fig. 4. Output power against the absorbed pump power for the 0.43 at.% Nd^{3+}-doped crystal sample.

the room-temperature absorption and emission spectra of the 0.43% Nd, Y-codoped:SrF_2 crystal, respectively. And the room-temperature absorption and emission spectra of the 0.15% Nd, Y-codoped:SrF_2 crystal are similar. The absorption peak is observed at 796 nm. The absorption cross sections for the crystals with Nd^{3+} doping concentrations of 0.43 and 0.15 at.% are 2.79×10^{-20} and 3.24×10^{-20} cm^2, respectively. We speculate the difference in the peak absorption cross sections for the two Nd concentrations as a result of broadening of the absorption lines. The emission peak exists at 1056 nm with stimulated cross section of 3.11×10^{-20} cm^2 for the crystal with Nd^{3+} doping concentration of 0.43 at.% and the stimulated cross section for the crystal with Nd^{3+} doping concentration of 0.15 at.% is almost the same. The gain bandwidth (full-width at half-maximum) is found to be 16 nm. The gain bandwidth and the properties of absorption and emission imply that the Nd, Y-codoped:SrF_2 crystals yield favorable laser performances.

In this letter, the laser performances of the TGT-grown Nd, Y:SrF_2 crystals are determined; thermal lens effect is assessed. The Nd^{3+} doping concentrations of the two uncoated samples are 0.15 and 0.43 at.%, respectively. The Y^{3+} doping concentrations of the samples are both 5 at.%. For the crystal sample with 0.43 at.% Nd^{3+} concentration, the pump absorption efficiency is 23%; for the crystal sample with 0.15 at.% Nd^{3+} concentration, the pump absorption efficiency is 19.7%. The maximum output power of the crystal sample with 0.43 at.% Nd^{3+} concentration is 1.023 W at 1056.9 nm; the slope and optical-to-optical conversion efficiencies are 53% and 45.9%, respectively. The focal length of the thermal lens is probed for the crystal sample with 0.15 at.% Nd^{3+} concentration. An improved cavity is designed by considering the thermal lens. Following the design, the maximum output power is 464 mW at 1056.9 nm and the slope efficiency is 36.1%. The wavelength is tuned from 1049.74 to 1059.13 nm

Experiments were initially conducted by using SrF_2 samples with 0.43 at.% Nd and 5 at.% Y to test their laser performances in CW operation (Fig. 3). The pump source was a fiber-coupled diode laser (nLIGHT Corporation) with a core diameter of 200 μm and numerical aperture (NA) of 0.22 that emits at a central wavelength of 793 nm at 26 °C. The maximum output power of the diode laser was 30 W. The pump beam was focused on the crystal using a series of lenses with an image ratio of 1:1. The laser cavity comprised a dichroic mirror M_1, a highly reflective concave mirror M_2 (radius of curvature, 400 mm), and a flat output coupler (OC) M_3. The diameter of pump beam inside the crystal was 260 μm based on the charge-coupled device (CCD) camera. The cavity (L_1, 250 mm; L_2, 400 mm) was designed with a mode size diameter of approximately 300 μm inside the

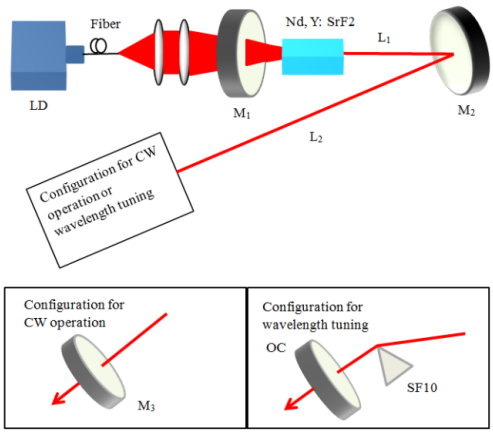

Fig. 3. Schematic diagram of the experimental setup.

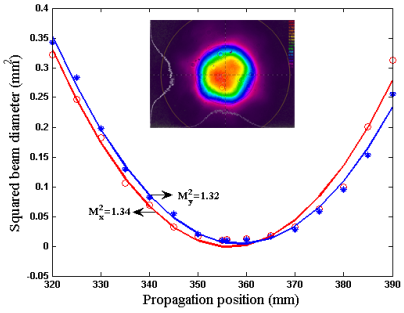

Fig. 5. M^2 factors for both directions perpendicular to the propagation axis for the 0.43 at.% Nd^{3+}-doped crystal sample. The inset shows the beam profile.

crystal to achieve a good mode matching. Both crystals with the same dimensions of 3×3×5 (mm) were wrapped with indium foil and mounted on a water-cooled copper block. The water temperature was maintained at 15 °C.

Figure 4 plots the output power against the absorbed pump power for the 0.43at.% Nd, 5 at.% Y:SrF_2 sample. To optimize the laser efficiency, the OC transmissions were 1%, 3%, and 7%. The highest efficiency and output power were achieved with 3% OC (condition of the TEM_{00} mode). The maximum output power of 1.023 W at 1056.9 nm was obtained with respect to the absorbed pump power of 2.23 W; the corresponding slope and optical-to-optical conversion efficiencies were 53% and 45.9%, respectively. The beam quality (M^2 factor) was measured in the highest output level when the pump power was 7.99 W (Fig. 5). The beam profile was then measured with a CCD camera (inset in Fig. 5). The results showed $M_x^2 = 1.34$ and $M_y^2 = 1.32$ in both directions perpendicular to the propagation axis. When the pump power was reduced to 6.59 W, the results were $M_x^2 = 1.32$ and $M_y^2 = 1.10$. Marked effects of the thermal lens were observed with high-pump power. For example, the output beam shape was distorted and exhibited higher order modes.

The pump power was reduced to 6.59 W to ensure a fundamental transverse mode output. Given this reduction, the crystal absorbed a power of 1.64 W. The tuning ability of the 0.43 at.% Nd-doped sample was then tested. An SF10 dispersive prism was introduced into the output arm of the laser cavity (Fig. 3). In the experiment, 3% OC was used to achieve an efficient tuning. The laser was tuned from 1049.74 to 1059.13 nm, of which the 1051–1054 nm range was not observed (Fig. 6). As can be seen from the emission spectrum (Fig. 2), there is a dip around the range of 1051–1054 nm. We speculate loss induced by the prism was too large for the range to oscillate. Two relatively narrow emission peaks occurred at approximately 1056.76 and 1058.34 nm in the tuning curve. Further tuning on a shorter wavelength was limited by the coating of the input coupler.

We apply the 0.15 at.% Nd-doped crystal sample in the cavity described above. The maximum output power of 339 mW at 1056.9 nm was obtained with respect to the absorbed pump power of 1.49 W and the beam quality (M^2 factor) was measured at the same time. The results showed $M_x^2 = 1.21$ and $M_y^2 = 1.17$ in both directions perpendicular to the propagation axis. Then we tried to improve the cavity design for a better beam quality.

The thermal lens effect of the crystal should be compensated to improve the output efficiency and beam quality. However, for the 0.43 at.% Nd-doped sample, it was broken due to a relatively high-pump power when measuring the dependence of focal length of thermal lens on the pump power. Hence, 0.15 at.% Nd-doped crystal sample was used in the succeeding experiments.

The thermal lens effect of the crystal is induced by increasing the pump power; the mode size in the crystal is reduced, and the stability region of the resonator is altered[13]. This effect generates higher order modes and decreases the output efficiency and beam quality[14]. To compensate the thermal lens effect, we obtained the focal length of the crystal for different pumping levels by measuring the beam size of the laser output. A resonator was then designed with insensitivity to the thermal lens effect.

A series of beam radii at different positions behind the OC was measured with a CCD camera. Subsequently, the beam radii on the OC were calculated by fitting the Gauss beam propagation equation as

$$\omega^2(z) = \omega_0^2\left[1 + \left(\frac{M^2\lambda z}{\pi\omega_0^2}\right)^2\right], \tag{1}$$

where M^2 is the M^2 factor. The focal lengths of thermal lenst were calculated from the Gauss beam transformation. The beam radii on the crystal were simultaneously obtained. We calculated the focal lengths of thermal lens and the beam radii on the 0.15 at.% Nd^{3+}-doped crystal. Figures 7 and 8 show the focal lengths of thermal lens and the beam radii on the crystal, respectively, with increasing absorbed pump power.

Specific criteria should be complied[14] to design the cavity with insensitivity to thermal effects. Firstly, the variations in the mode size induced by the thermal lens effect should be as small as possible. Secondly, the

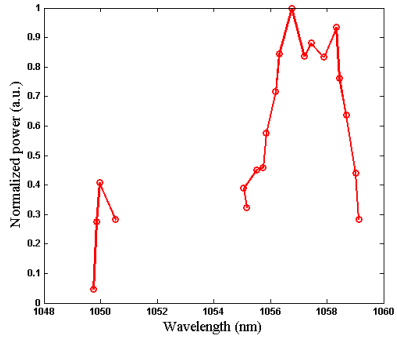

Fig. 6. Wavelength tuning in the CW regime for the 0.43 at.% Nd^{3+}-doped crystal sample.

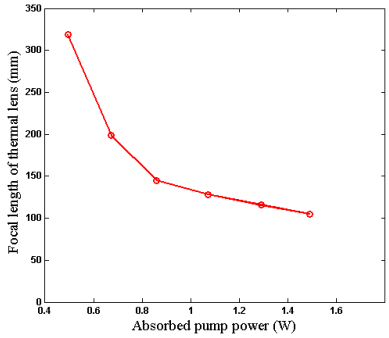

Fig. 7. Focal length of thermal lens against the absorbed pump power for the 0.15 at.% Nd^{3+}-doped crystal sample.

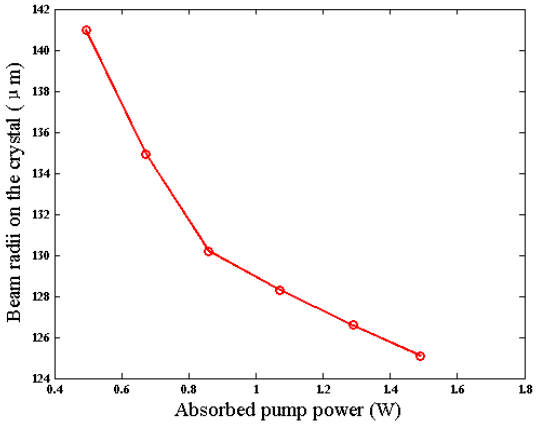

Fig. 8. Beam radii on the crystal against the absorbed pump power for the 0.15 at.% Nd^{3+}-doped crystal sample.

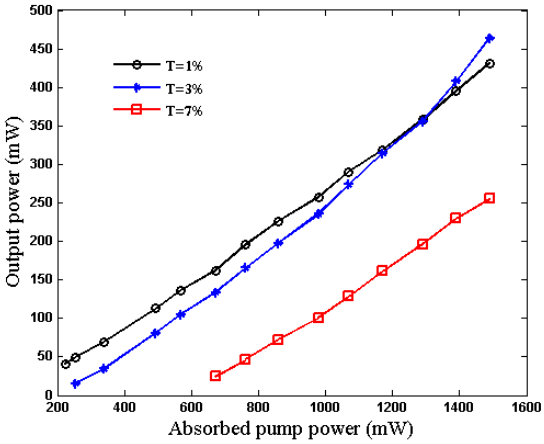

Fig. 10. Output power against the absorbed pump power for the 0.15 at.% Nd^{3+}-doped crystal sample.

stability region of the resonator should be less sensitive to this effect. Given the focal lengths of thermal lens of the sample crystal, the cavity was improved from the two criteria: L_1 was changed to 220 mm and the other parameters were unchanged (Fig. 3). Figure 9 shows the stimulated beam radii on the crystal varying with focal lengths of thermal lens of the crystal. The result indicates that the beam radius remains acceptable even if the focal length of thermal lens is as small as 60 mm.

To optimize the laser efficiency, various OC transmissions (1%, 3%, and 7%) were used. The maximum efficiency and output power were obtained with 3% OC. The maximum output power was 464 mW at 1056.9 nm with respect to the absorbed pump power of 1.49 W. The corresponding slope efficiency and optical-to-optical conversion efficiencies were 36.1% and 31.1%. Figure 10 shows the laser performances in the CW operation for the Nd^{3+}-doped crystal sample with a TEM_{00} mode output.

The M^2 factor and the beam profile in the high-power pumping situation were close to the diffraction limit. For a pumped power output of 6.59 W, the 0.15 at.% Nd^{3+}-doped crystal sample absorbs 1.49 W and yields beam qualities of $M_x^2 = 1.04$ and $M_y^2 = 1.06$. Figure 11 shows the measurement results for the M^2 factor; the inset of Fig. 11 shows the beam profile measured with a CCD camera, which indicates a perfect TEM_{00} mode.

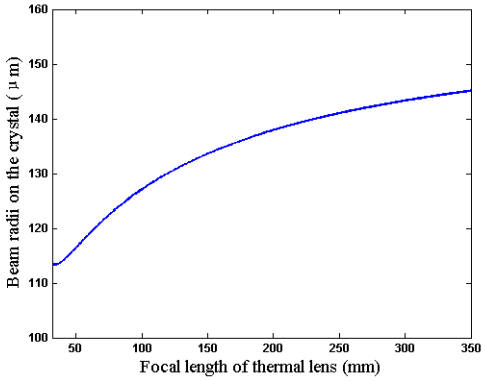

Fig. 9. Stimulated beam radii on the crystal as a function of the focal lengths of thermal lens of the crystal.

The output power for the crystal sample with 0.43 at.% Nd^{3+} concentration at 1.49 W absorbed power was more than 0.6 W, considerably larger than for the one with 0.15 at.% Nd^{3+} concentration at the same absorbed power in the optimized cavity. The output efficiency of the crystal sample with a 0.15 at.% Nd^{3+} doping concentration was about 20% lower than the sample with a 0.43 at.% Nd^{3+} doping concentration. The lower efficiency of the less concentrated sample was caused by more losses due to larger angle between L_1 and L_2. However, the beam quality of the 0.15 at.% Nd^{3+}-doped crystal sample enhances at the same pump power based on its weak thermal lens effect. This could be attributed to the lower doping concentration and improved cavity designs. Wavelength tuning results of this sample was very similar to that of 0.43 at.% Nd^{3+}-doped crystal, also with the range of 1051–1054 nm not observed. It can be speculated that crystals with Nd^{3+} doping concentrations between 0.15 and 0.43 at.% would have better laser performances in the improved cavity, both in output efficiency and beam quality.

In conclusion, we analyze the laser properties of TGT-grown Nd, Y:SrF_2 crystals with Nd^{3+} concentrations of 0.43 and 0.15 at.%, and Y^{3+} concentration of 5 at.%. The uncoated crystal samples with similar lengths of 5 mm are pumped by the 793 nm LD. For the 0.43 at.% Nd^{3+}-doped crystal sample, the maximum output power is 1.023 W at 1056.9 nm based on the absorbed pump power of 2.23 W. The corresponding slope and optical-to-optical conversion efficiencies are 53% and 45.9%. The focal lengths of thermal lens formed during operation and the beam radii on the crystal are investigated for the 0.15 at.% Nd^{3+}-doped crystal sample. The improved cavity for this crystal sample is designed from the focal lengths of the thermal lens. The

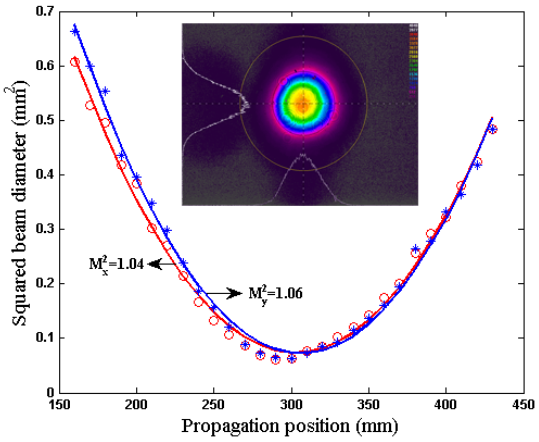

Fig. 11. M^2 factors for both directions perpendicular to the propagation axis for the 0.15 at.% Nd^{3+}-doped crystal sample. The inset shows the beam profile.

maximum output power is found to be 464 mW with respect to the absorbed pump power of 1.49 W. The slope and optical-to-optical conversion efficiencies are 36.1% and 31.1%, respectively. The beam quality of the 0.15 at.% Nd^{3+}-doped crystal sample with an improved cavity is good. Wavelength tuning is also investigated. The tuning ranges from 1049.74 to 1059.13 nm. The experiments prove that the Nd, Y:SrF_2 crystal can be a potentially efficient laser material.

This work was supported by the National Natural Science Foundation of China under Grant No. 61378030.

References

1. U. Keller, Nature 424, 831 (2003).
2. Y. Xu, J. W. Y. Huang, Y. Li, X. Lu, and Y. Leng, High Power Laser Sci. Eng. **1,** 98 (2013).
3. X. Fu, J. Li, and X. Liang, Chin. Opt. Lett. **11,** 081401 (2013).
4. T. Lu, J. Wang, X. Zhu, R. Zhu, H. Zang, and W. Chen, Chin. Opt. Lett. **11,** 051402 (2013).
5. Y. E. Kariss and P. Feofilov, Optika i Spektroskopiya **14,** 169 (1963).
6. L. F. Johnson, J. Appl. Phys. **34,** 897 (1963).
7. A. A. Kaminski, V. V. Osico, A. M. Prochoro, and Y. K. Voronko, Phys. Lett. **22,** 419 (1966).
8. Y. K. Voronko, A. A. Kaminski, and V. V. Osiko, Sov. Phys. JETP-USSR **22,** 295 (1966).
9. S. A. Payne, J. A. Caird, L. L. Chase, L. K. Smith, N. D. Nielsen, and W. F. Krupke, J. Opt. Soc. Am. B-Opt. Phys. **8,** 726 (1991).
10. J. Liu, M. W. Fan, L. B. Su, D. P. Jiang, F. K. Ma, Q. Zhang, and J. Xu, Laser Phys. **24,** 035802 (2014).
11. M. Jelinek, V. Kubecek, L. Su, D. Jiang, F. Ma. Q. Zhang, Y. Cao, and J. Xu, Laser Phys. Lett. **11,** 055001 (2014).
12. Z. P. Qin, G. Q. Xie, J. Ma, W. Y. Ge, P. Yuan, L. J. Qian, L. B. Su, D. P. Jiang, F. K. Ma, Q. Zhang, Y. X. Cao, and J. Xu, Opt. Lett. **39,** 1737 (2014).
13. J. Steffen, J. P. Lortsche, and G. Herziger, IEEE J. Quant. Electron. **8,** 239 (1972).
14. V. Magni, Appl. Opt. **25,** 107 (1986).